OPAL Physics Note PN247
6^{th} August 1996

A Measurement of the Average Bottom Hadron Lifetime

The OPAL Collaboration

Abstract

The average b hadron lifetime, τ_b, has been measured using data collected with the OPAL detector between 1991 and 1994. A lifetime tag based on a neural network algorithm was used to select $Z^0 \to b\bar{b}$ events. A reconstructed secondary vertex on the away side from the b-tag was used to measure the b hadron decay length. This was combined with an estimate of the b hadron momentum, allowing the b hadron decay time to be evaluated. A fit to the 95 620 reconstructed decay times yields :

$$\tau_b = (1.597 \pm 0.010\,(\text{stat}) \pm 0.026\,(\text{syst}))\ \text{ps}.$$

This note describes preliminary OPAL results and is intended primarily for members of the collaboration.

1 Introduction

Two main techniques are used to measure the average b hadron lifetime, τ_b, at LEP energies. The first and most widely adopted method uses maximum likelihood fits to the distribution of the impact parameters of leptons from semileptonic b hadron decays [1], where the impact parameter is the distance of closest approach of the lepton to the interaction point. Previous measurements of τ_b by the OPAL collaboration used this technique. The result, $\tau_b = 1.523 \pm 0.034\,(\text{stat}) \pm 0.038\,(\text{syst})$ ps, was measured from data collected between 1990 and 1991 [2]. The second method uses inclusively reconstructed secondary vertices to estimate the decay length of the b hadron [3]. It is interesting to compare results from these two techniques, as the systematic errors are largely uncorrelated. In particular, there is no reliance on the modelling of semileptonic b hadron decays in the second method. This is the method used in the analysis described in this paper.

This paper is organised as follows. A brief description of the OPAL detector is given in section 2. The data samples and selection procedure are presented in section 3. The analysis method is described in section 4 and the procedure used to select $Z^0 \to b\bar{b}$ events is detailed in section 5. Section 6 describes the procedure for reconstructing the b hadron decay time. The fitting techniques used to extract the lifetime are defined in sections 7 and 8. The results and systematic error studies are detailed in sections 9 and 10 respectively. Finally, the results are summarised and compared to other contemporary results in section 11.

2 The OPAL Detector

The OPAL detector was used to collect data from decays of the Z^0 boson, produced in e^+e^- collisions at the LEP collider at CERN. The OPAL detector is equipped with a central tracking system comprising a silicon microvertex detector, a precision vertex drift chamber, a large volume jet chamber and z-chambers. It is positioned inside a solenoid that provides a uniform magnetic field of 0.435 T. The coil is surrounded by a lead-glass electromagnetic calorimeter with a presampler, a hadron calorimeter and muon chambers. A detailed description of the whole detector can be found elsewhere [4]. The most important component for this analysis is the central tracking system. The jet chamber provides tracking and ionization energy loss ($\mathrm{d}E/\mathrm{d}x$) measurements [5], and is surrounded by a set of chambers to measure the z-coordinate[a] of tracks as they exit the jet chamber. In 1991, a high precision silicon microvertex detector [6] was installed around the beryllium-composite beam pipe at the interaction point. In 1993, the silicon detector was upgraded [7] to supply additional tracking information in the z-coordinate, but only r-ϕ silicon microvertex detector information is used for the analysis described in this paper. The impact parameter resolution in the x-y plane achieved for 45 GeV/c tracks in $Z^0 \to \mu^+\mu^-$ events is 18 μm for tracks with associated hits in each of the two layers of the silicon microvertex detector.

3 Data Samples and Selection Procedure

This analysis was performed on data collected in the vicinity of the Z^0 peak between 1991 and 1994 with the silicon microvertex detector operational. Hadronic Z^0 decays were selected using criteria described in a previous publication [8], where the selection efficiency was measured to

[a] In the OPAL right-handed coordinate system the x-axis points towards the centre of the LEP ring, the y-axis points upwards and the z-axis points in the direction of the electron beam. The polar angle θ and the azimuthal angle ϕ are defined with respect to z and y, respectively, while r is the distance from the z-axis.

be (98.4±0.4)%. The central tracking system and electromagnetic calorimeters were required to have been fully operational when the data were collected.

Monte Carlo events were generated using the JETSET 7.4 program [9] with parameters tuned to OPAL data [10]. The production rates of b hadrons were in the ratio B^0:B^+:B_s:b baryon = 40:40:12:8, and the lifetimes of B mesons and b baryons were set to 1.6 ps and 1.2 ps respectively. These lifetimes are consistent with the 1996 PDG averages [11], which give : $\tau(B^+) = 1.62 \pm 0.06$ ps, $\tau(B^0) = 1.56 \pm 0.06$ ps, $\tau(B_s) = 1.61^{+0.10}_{-0.09}$ ps and an average b baryon lifetime of 1.14 ± 0.08 ps. The fragmentation function of Peterson et al. [12] was used for the b quarks. Two types of Monte Carlo sample are used in this analysis. In the default sample ε_b =0.004, which corresponds to a mean scaled energy of $\langle x_E \rangle$=0.703 for the weakly-decaying b hadron. In the 'modified fragmentation' sample, ε_b =0.006, resulting in $\langle x_E \rangle$=0.680. Recent measurements [13] give $\langle x_E \rangle$=0.701±0.008, indicating that the default sample provides better modelling of the b fragmentation properties. To simulate detector response, the Monte Carlo event samples were passed through the detector simulation program [14] . Comparisons between data and Monte Carlo revealed significant discrepancies in the tails of impact parameter distributions. For the default samples, an *ad hoc* smearing procedure was applied to the impact parameter and ϕ measurements in order to bring these distributions into agreement. In this procedure, for 8.5% of the tracks (chosen at random) the impact parameters were smeared by 1.5 σ, and a further 1% of tracks had their impact parameters smeared by 8.5 σ, where σ represents the estimated uncertainty on the impact parameter from the fitted track parameters. Event samples without this *ad hoc* smearing were also used, referred to as 'unsmeared' in this paper.

4 Analysis Method

Each event was divided into two hemispheres using the thrust axis of the event. Hemispheres were tagged as containing candidate b hadrons ('b-tagged') using secondary vertices reconstructed with the algorithm described in [15]. Properties of such secondary vertices were used as inputs to a neural network algorithm that was trained to select $Z^0 \to b\bar{b}$ events [16]. According to Monte Carlo studies, this procedure results in a sample that is approximately 96% pure in $Z^0 \to b\bar{b}$ events for an efficiency of about 17%.

Charged tracks and electromagnetic clusters not associated with a charged track were resolved into jets using a 'cone' algorithm [17]. The size of the cone was chosen to include nearly all the decay products of a b hadron into one jet. The jets also include particles produced in the fragmentation process which originate from the e^+e^- collision point. Only events with exactly two jets were used in this analysis to reduce the number of events where both b quarks are in the same hemisphere due to the emission of an energetic gluon.

The hemisphere opposite a b-tag was searched for secondary vertices using a vertexing algorithm (described in section 6) which was more suited to measuring accurate decay lengths, rather than just providing a b-tag. The primary event vertex was reconstructed using the charged tracks in the event, constrained by the average position and spread of the e^+e^- collision point. The decay length between the primary event vertex and the secondary vertex (opposite from the b-tag) was converted into a decay time using an estimate of the b hadron momentum. The average b hadron lifetime was extracted from a fit to the distribution of reconstructed decay times.

5 Selecting $Z^0 \to b\bar{b}$ Events and Purity Determination

Candidate $Z^0 \to b\bar{b}$ events were selected by using seven parameters of secondary vertices reconstructed using the algorithm described in [15] as inputs to a neural network algorithm [16]. The

most important inputs are the decay length, its uncertainty and the vertex multiplicity. The neural network allows a very high purity sample of $Z^0 \to b\bar{b}$ events to be isolated.

The double tagging technique described in [18] was used to determine the hemispheric b purity in data. This avoids unnecessary dependence on Monte Carlo modelling. The number of singly tagged hemispheres, N_v, and the number of events with two tagged hemispheres, N_{vv}, in a sample of $N_{\rm had}$ hadronic events can be expressed as :

$$N_v = 2\left(\epsilon_{\rm b}\frac{\Gamma_{\rm b\bar{b}}}{\Gamma_{\rm had}} + \epsilon_{\rm c}\frac{\Gamma_{\rm c\bar{c}}}{\Gamma_{\rm had}} + \epsilon_{\rm uds}\frac{\Gamma_{\rm u\bar{u}}+\Gamma_{\rm d\bar{d}}+\Gamma_{\rm s\bar{s}}}{\Gamma_{\rm had}}\right)N_{\rm had}\ ; \tag{1}$$

$$N_{vv} = \left(C_{\rm b}\epsilon_{\rm b}^2\frac{\Gamma_{\rm b\bar{b}}}{\Gamma_{\rm had}} + \epsilon_{\rm c}^2\frac{\Gamma_{\rm c\bar{c}}}{\Gamma_{\rm had}} + \epsilon_{\rm uds}^2\frac{\Gamma_{\rm u\bar{u}}+\Gamma_{\rm d\bar{d}}+\Gamma_{\rm s\bar{s}}}{\Gamma_{\rm had}}\right)N_{\rm had}. \tag{2}$$

The quark partial widths are denoted by $\Gamma_{\rm q\bar{q}}/\Gamma_{\rm had}$, and Standard Model values were used for the up and down quark types, respectively [19]. The hemispheric tagging efficiencies for $b\bar{b}$, $c\bar{c}$ and lighter quark events are denoted by $\epsilon_{\rm b}, \epsilon_{\rm c}$ and $\epsilon_{\rm uds}$, respectively. The values of $\epsilon_{\rm b}$ and $\epsilon_{\rm c}$ were extracted from the data by solving equations 1 and 2 simultaneously, while $\epsilon_{\rm uds}$ was obtained from Monte Carlo. The coefficient $C_{\rm b}$ describes the efficiency correlation between hemispheres in a $b\bar{b}$ event. This is needed because the tagging probabilities for the two hemispheres are not just correlated through the flavour of the initial quark pair. This coefficient is only evaluated for $b\bar{b}$ events as the $b\bar{b}$ event fraction is dominant. The numerical value of $C_{\rm b}$ differs from unity for three main reasons : (i) the reconstructed position and uncertainty of the primary vertex are common to both hemispheres; (ii) the emission of an energetic gluon can cause both the b and $\bar{\rm b}$ jets to fall into one hemisphere, and gluon emission also produces a small correlation between the b and $\bar{\rm b}$ hadron's momenta; (iii) the b and $\bar{\rm b}$ hadrons are usually produced back-to-back, so geometrical correlations will therefore be produced if the tagging efficiency is not uniform over the geometrical acceptance of the detector. The relationship

$$C_{\rm b} = \frac{\epsilon_{\rm b}^{vv}}{(\epsilon_{\rm b})^2}, \tag{3}$$

was used to evaluate $C_{\rm b}$, where $\epsilon_{\rm b}^{vv}$ is the double tagging efficiencies for $b\bar{b}$ events, evaluated from Monte Carlo. The b purity, $P_{\rm b}$, can be determined using the relationship

$$P_{\rm b} = \frac{2\,\epsilon_{\rm b}N_{\rm had}}{N_v}\cdot\frac{\Gamma_{\rm b\bar{b}}}{\Gamma_{\rm had}}\ . \tag{4}$$

Values of $C_{\rm b}$=(0.970$\pm$0.007) and $\epsilon_{\rm uds}$=(0.058$\pm$0.002)% were determined from the default Monte Carlo samples. The quoted errors are statistical. The true value of the b purity in the Monte Carlo was $P_{\rm b}$ = 95.8%. The true values of the c and uds purities were 3.1% and 1.1%, respectively. These values of $C_{\rm b}$ and $\epsilon_{\rm uds}$ were used with 1991–1994 data to determine $P_{\rm b} = (94.6 \pm 0.5)\%$, where the uncertainty includes the error on $C_{\rm b}$.

6 Reconstructing the Decay Time

The hemisphere opposite a b-tag was searched for secondary vertices. The vertexing algorithm works in the r-ϕ plane to select tracks and to fit the position of the secondary vertex. The two precisely measured tracks (requiring hits in either the silicon microvertex or vertex drift chambers) with the most significant separation from the primary event vertex were taken as seed tracks. Precisely measured tracks that were at least three standard deviations from the primary vertex were also taken as seeds. Separated vertex candidates were formed by considering all possible pairs of seed tracks to form a vertex nucleus. Other tracks were added to this

nucleus vertex provided they matched this vertex better than the primary vertex, and the vertex probability was >1%. If more than one candidate secondary vertex was found by the algorithm, a single secondary vertex was chosen, based on the number of tracks associated to each vertex and the reconstructed vertex positions. The decay length in the r-ϕ plane was calculated for each vertex from a fit to the primary vertex position and the seed vertex position. The r-ϕ vector momentum sum of the vertex tracks was used to constrain the decay length direction. Such a constraint was also used in a measurement of the decay length in 3-prong τ decays [20]. When fitting the decay length the uncertainty from the primary vertex position is usually negligible, with the dominant errors arising from uncertainties in the track parameters for the seed vertex and the choice of tracks.

Reconstructed secondary vertices consisting of just two charged tracks were not used in this analysis, as they suffered from large combinatorial backgrounds and therefore behaved in a systematically different manner from other secondary vertex multiplicities. Two-track vertices formed 17% of both the Monte Carlo and data samples.

A set of quality requirements was imposed on the secondary vertices used to form the decay length measurement in order to suppress badly reconstructed vertices, where the reconstructed decay length is only weakly correlated with the true decay length. Following the prescription described in [21], the following selection criteria were tuned for this analysis using the default Monte Carlo sample.

- The transverse miss distance divided by its error is required to be less than three. The transverse miss distance is defined as the distance between the primary and secondary vertices projected onto an axis orthogonal to the summed momentum vector of tracks associated with the secondary vertex. This condition helps to remove secondary vertices formed from random track combinations.

- The decay length error (calculated from the parameters of the tracks making up the secondary vertex) was required to be less than 0.06 cm.

- The invariant mass of the secondary vertex tracks (assuming pion masses) was required to be greater than 0.8 GeV/c^2.

- For negative decay lengths, the secondary vertex was rejected if it was more than two standard deviations from the primary vertex. The sign of the decay length was assigned according to the scalar product of the jet direction and the decay length vector.

Table 1 shows the effect of each quality requirement on the efficiency for reconstructing a good secondary vertex from a b hadron decay. The overall efficiency for reconstructing a secondary vertex from b hadron decay that passed all the selection criteria was measured from Monte Carlo

Quality Requirement	Efficiency Loss
Vertex with $\geq$ 3 tracks	20%
Transverse miss distance significance $<$ 3	7%
Decay length error $<$ 0.06 cm	6%
Vertex mass $>$ 0.8 GeV/c^2	4%
Decay length significance $>$ -2	2%
Total	34%

Table 1: The effect of each quality requirement on the efficiency for identifying secondary vertices from b hadron decays in Monte Carlo.

to be 66%. The equivalent efficiency for reconstructing a secondary vertex in a non-b$\bar{\text{b}}$ event selected by the b-tag was estimated to be 51%.

The decay length, L, was estimated from the reconstructed decay length in the $r-\phi$ plane, $\ell_{r\phi}$, using

$$L = \frac{\ell_{r\phi}}{\sin\theta} \,, \tag{5}$$

where θ is the polar angle of the b hadron, estimated using the jet axis. The uncertainty on $\sin\theta$ is negligible compared to the uncertainty in the two-dimensional decay length and therefore leads to a negligible additional error on the calculation of the three-dimensional decay length. After all the quality requirements, the distribution of reconstructed decay length less the true decay length was well centred with a mean of 0.02 cm and a full width at half maximum (called the central width) of 0.13 cm.

The technique used to calculate the boost needed to convert the decay length measurement into a decay time was similar to that used in studies of B meson oscillations [21] and B** production [22] by the OPAL collaboration. The event was treated as a two-body decay of the Z^0, of mass $\mathrm{M} = 91.2\,\mathrm{GeV}/c^2$ [19]. The two decay bodies are the b jet, of mass m_{bjet} and momentum p, and the rest of the event, of mass m_{rest} and momentum -p. The following relationship due to energy conservation can be used to estimate the energy of the b jet, E_{bjet} :

$$E_{\mathrm{bjet}} = \frac{\mathrm{M}^2 + m_{\mathrm{bjet}}^2 - m_{\mathrm{rest}}^2}{2\mathrm{M}} \,. \tag{6}$$

The mass of the b jet was assumed to be the mass of the $\mathrm{B}^{\pm}$, B^0 meson, $5.28\,\mathrm{GeV}/c^2$ [19]. Monte Carlo studies showed that the final b hadron decay time estimate is insensitive to the choice of b jet mass. The mass of the rest of the event was calculated from the energy and momentum of charged tracks, assuming pion masses, and unassociated electromagnetic clusters, assuming zero mass, not assigned to the b jet.

If the total fragmentation energy in the b jet is denoted by E_{bfrag}, then the energy of the b hadron, E_{b}, is given by

$$E_{\mathrm{b}} = E_{\mathrm{bjet}} - E_{\mathrm{bfrag}} \,. \tag{7}$$

Charged tracks are classified as coming from b decay or b fragmentation using a neural network algorithm. Unassociated electromagnetic clusters are similarly classified using angular information. The following four parameters were used to classify each track presented to the neural network.

- The d_0 significance (d_0/σ_{d_0}) with respect to the primary vertex, where d_0 is the impact parameter in the $x-y$ plane, and σ_{d_0} denotes the error on d_0. The sign of d_0 is chosen to be positive if the point of closest approach of the track to the primary vertex, in the $x-y$ plane, is in the same hemisphere as the jet containing the track, otherwise it is negative.
- The d_0 significance with respect to the secondary vertex.
- The track momentum.
- The value of $\cos\Theta$, where Θ is the angle between the track and the jet axis.

Each of these parameters is shown for tracks from b decay and b fragmentation in figure 1. The neural network was trained on Monte Carlo events to discriminate between tracks from b decay and b fragmentation. The output of the neural network for these two sources of tracks is also shown in figure 1. Monte Carlo studies showed that the best charged b fragmentation energy

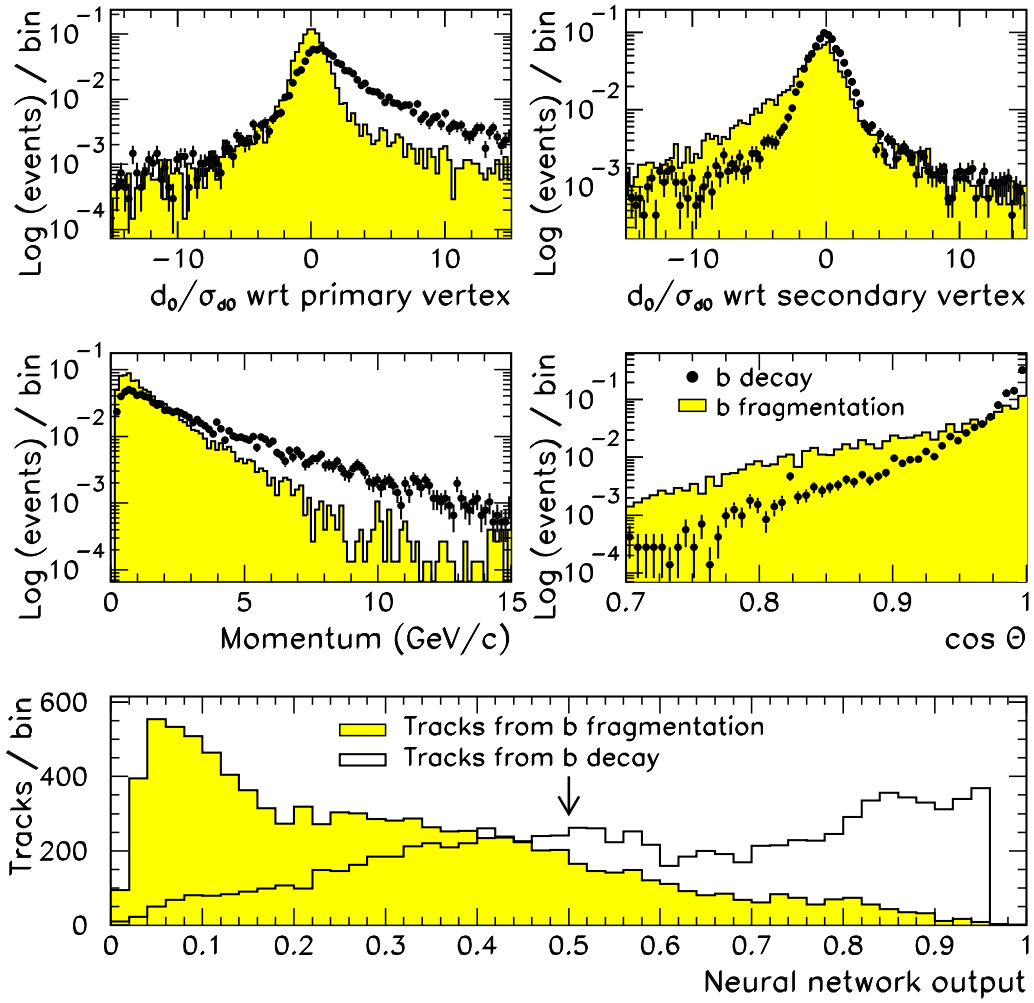

Figure 1: The upper four plots show the input parameters to the neural network, used to discriminate between tracks from b hadron decay and from b fragmentation. The points represent tracks from b hadron decay and the shaded areas represent tracks from fragmentation in $Z^0 \to b\bar{b}$ events. All distributions are normalised to unit area. The output of the neural network for tracks from b hadron decay and fragmentation in $Z^0 \to b\bar{b}$ events is also shown. A neural network output <0.5, indicated by the arrow, was used to select tracks from fragmentation.

resolution was obtained when a neural network output of less than 0.5 was used to select tracks from fragmentation.

The neutral fragmentation energy was much harder to identify. Only the angle of the unassociated electromagnetic cluster relative to the jet axis, $\cos\Theta$, was used. The range of $\cos\Theta$ was split into three : $\cos\Theta \leq 0.850$ – b fragmentation; $\cos\Theta \geq 0.965$ – b decay; and $0.965 < \cos\Theta < 0.850$ – weighted, where the cluster energy is shared between the b fragmentation (55%) and b hadron (45%) energy sums. These ranges were tuned to optimise the b hadron energy resolution after the charged fragmentation energy resolution had been optimised.

Using the estimates of the b jet and b fragmentation energies, the b hadron energy was determined and compared to the true value from Monte Carlo. These studies showed that the b hadron energy resolution could be improved when the mass of the rest of the event, $m_{\rm rest}$, was scaled by a factor 87 GeV / $E_{\rm vis}$, where $E_{\rm vis}$ is the total visible energy in the event. The

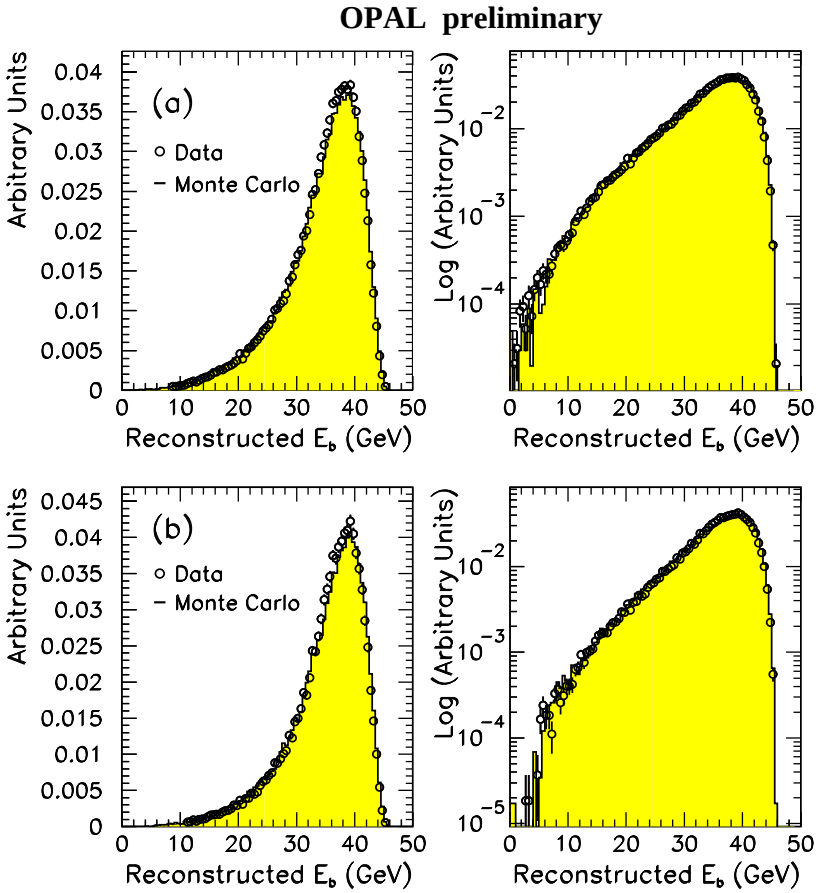

Figure 2: The reconstructed b hadron energy in Monte Carlo compared to that in data for : (a) all decay times and (b) reconstructed decay times > 1 ps, where the energy resolution is improved.

resulting distribution of the b hadron energy resolution has a central width of 8 GeV and is well centred, with a mean of 0.03 GeV. Figure 2 shows the reconstructed b hadron energy in Monte Carlo compared to that in data for all decay times and for reconstructed decay times > 1 ps, where the energy resolution is improved. The distributions have been normalised to each other and agree well, but small imperfections in the Monte Carlo description of the data are addressed as systematic errors.

The reconstructed decay time, t, of a b hadron was evaluated by combining the three-dimensional decay length, L, and the b hadron energy estimate, E_{b}, with the estimated mass of the b hadron, m_{b} :

$$t = \frac{m_{\mathrm{b}}\, L}{\sqrt{E_{\mathrm{b}}^2 - m_{\mathrm{b}}^2}}\,, \tag{8}$$

where m_{b} was chosen to be 5.28 GeV/c^2. In cases where $E_{\mathrm{b}} < m_{\mathrm{b}}$, the event was discarded. Figure 3a shows the correlation between true and reconstructed decay times. The decay time resolution shown in figure 3b has a central width of 0.8 ps and is well centred about zero.

In the next section the technique used to extract the average b hadron lifetime from the reconstructed decay time distribution is discussed.

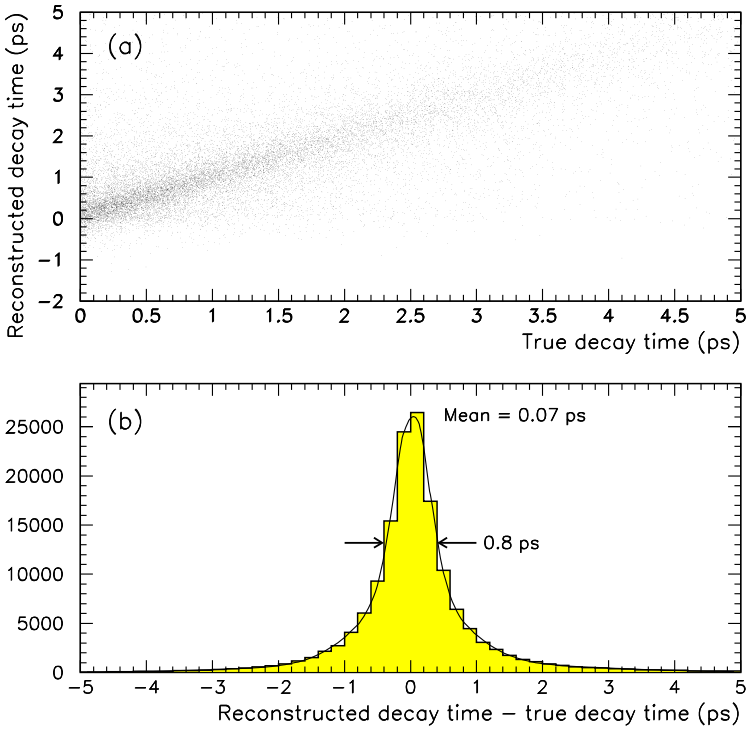

Figure 3: Plot (a) shows the correlation between reconstructed and true b hadron decay times. Plot (b) shows the decay time resolution. Both plots are from Monte Carlo events.

7 Likelihood Fit

A binned maximum likelihood fit may be used to extract τ_b from the distribution of reconstructed decay times. The distribution of reconstructed decay times can be parametrised using : (i) a physics function, which describes the distribution of true decay times as a function of τ_b; (ii) a signal resolution function, which describes the distribution of reconstructed decay times, from real b hadron decays, for a given true decay time; and (iii) a background resolution function, which describes the reconstructed decay time distribution of non-$b\bar{b}$ events.

The likelihood function, $\mathcal{L}$, can be defined for N reconstructed decay times, t_i, as

$$\mathcal{L}(\tau_b, \vec{a}) = \prod_{i=1}^{N} \mathbb{P}(t_i; \tau_b, \vec{a}), \tag{9}$$

where

$$\vec{a} = \vec{a_p} + \vec{a_s} + \vec{a_b}. \tag{10}$$

The normalised probability density function, $\mathbb{P}$, is a function of τ_b, t_i, and the parameters needed to describe the physics, signal resolution and background resolution functions, denoted by $\vec{a_p}$, $\vec{a_s}$ and $\vec{a_b}$, respectively. The estimate of τ_b that makes the data most likely is given by the maximum value of $\mathcal{L}$. The precise form of $\mathbb{P}$ is

$$\mathbb{P}(t_i; \tau_b, \vec{a}) = z \int_0^\infty \mathcal{P}(t', \tau_b, \vec{a_p}) \mathcal{R}_{sig}(t_i, t', \vec{a_s})\, dt' + (1 - z)\mathcal{R}_{bkgd}(t_i, \vec{a_b}) \ , \tag{11}$$

where t' represents the true decay time. The physics function is denoted by $\mathcal{P}$ and the signal and background resolution functions by $\mathcal{R}_{\rm sig}$ and $\mathcal{R}_{\rm bkgd}$, respectively. Each of the functions is individually normalised to unity. The parameter z describes the amount of signal in the fitted sample. It was derived using the double tagging technique described in section 5 with two corrections. The first correction reduces the background by a factor 0.76 to account for the lower efficiency for the background events to pass the vertex selection cuts, as described in section 6. The second correction reduces z by 0.0033, derived from Monte Carlo, to account for the additional background of events with two b quarks in the same hemisphere due to the emission of an energetic gluon. This additional background is highly suppressed since only events with exactly two jets are used in this analysis. The resulting value is $z = 0.956 \pm 0.006$, where systematic uncertainties of 25% and 50% have been assigned to the two corrections, respectively.

In the following sections the exact forms of each of the constituent parts of the likelihood function are described in more detail.

7.1 Physics Function

The physics function, which describes the distribution of true decay times as a function of $\tau_{\rm b}$, is given by

$$\mathcal{P}(t', \tau_{\rm b}, \vec{a_{\rm p}}) = \frac{1}{\tau_{\rm b}} \exp(-t'/\tau_{\rm b}) \frac{1}{F(t', \vec{a_{\rm p}})\,\mathcal{N}(\vec{a_{\rm p}})}, \tag{12}$$

where

$$F(t', \vec{a_{\rm p}}) = \exp(a + bt') + c, \tag{13}$$

$$\vec{a_{\rm p}} = \{a, b, c\} \tag{14}$$

and

$$\mathcal{N}(\vec{a_{\rm p}}) = \int_0^\infty \frac{1}{\tau_{\rm b}} \exp(-t'/\tau_{\rm b}) \frac{1}{F(t', \vec{a_{\rm p}})}\, dt'. \tag{15}$$

As well as a lifetime exponential, the physics function contains a correction function, F, which is used to account for biases in the true decay time distribution at small decay times. The bias corrected physics function is normalised by the function $\mathcal{N}$. The integration is performed numerically. The bias arises from two independent sources:

1. Secondary vertex selection. This effect dominates, and shifts the mean of the true decay time distribution by +0.09 ps. The efficiency for detecting a secondary vertex that passes all the quality requirements decreases as the true decay time tends towards zero.

2. Neural network b-tagging. This shifts the mean of the true decay time distribution by −0.03 ps. The primary vertex is common to both hemispheres and tagged events tend to have a smaller than average primary vertex error. The primary vertex error will be reduced when there are more tracks available for the primary vertex fit. This is more likely when the mean decay length, and hence the true decay time, is small.

The bias correction function, F, is derived from Monte Carlo from the ratio between the true decay time distributions before and after the application of the b-tagging and secondary vertex selection. The distribution of F is well parameterised using the parameter values shown in figure 4. The bias mainly affects the region $t' < 1$ ps.

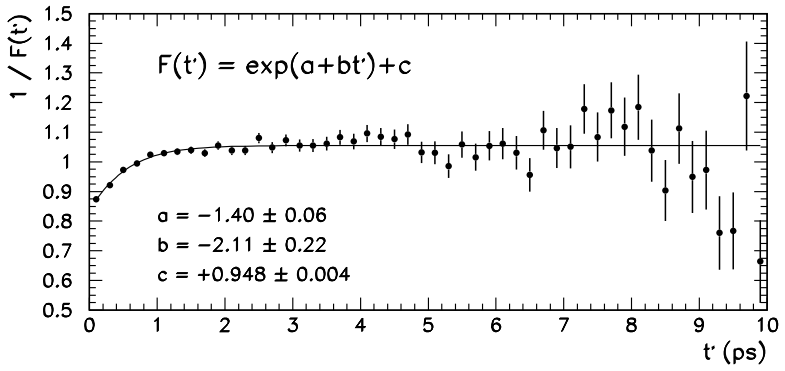

Figure 4: The bias correction function, $1/F$, as a function of true decay time. The bias mainly affects the region $t' < 1$ ps. The fitted parameter values are shown.

7.2 Signal Resolution Function

The reconstructed decay time deviates from the true decay time due to imperfect secondary vertex reconstruction and b hadron energy estimation. The relationship between the reconstructed and true decay times is not trivial, and depends on the value of the true decay time. The default Monte Carlo sample was used to parametrise the resolution function which describes the distribution of reconstructed decay times for a given true decay time.

The shape of the reconstructed decay time distribution predicted by the resolution function varies with true decay time, as shown in figure 5 for six slices of true decay time. The enhanced number of events around zero in reconstructed decay time for large true decay times are due to events where the reconstructed secondary vertex consists partially or totally of tracks that originate from the primary vertex. The form of the resolution function is therefore rather complicated as it must account for the peaks in the reconstructed decay time distribution around both zero and the true decay time.

The precise form of the resolution function is

$$\mathcal{R}_{\rm sig}(\mathrm{t}, \mathrm{t}', \vec{\mathrm{a}_{\rm s}}) = (1 - \mathrm{f}\ \exp(-\mathrm{w}\,\mathrm{t}'))\Big(\mathrm{g}\,\mathcal{G}_1 + (1-\mathrm{g})\,\mathcal{G}_2\Big) + \mathrm{f}\ \exp(-\mathrm{w}\,\mathrm{t}')\Big(\mathrm{h}\,\mathcal{G}_3 + (1-\mathrm{h})\,\mathcal{G}_4\Big), \tag{16}$$

where $\mathcal{G}_{\rm n}$ represents a normalised Gaussian. The parameters f, g and h are restricted to the range $0 < \{\mathrm{f},\ \mathrm{g},\ \mathrm{h}\} < 1$, and describe the relative fraction of each Gaussian such that the resolution function as a whole remains normalised. The Gaussians are described by

$$\underset{\mathrm{n}=1,2}{\mathcal{G}_{\rm n}} = \frac{1}{\sqrt{2\pi}\,\sigma_{\rm n}} \exp\left(-\frac{1}{2}\left(\frac{\mathrm{t} - \mathrm{j_n}\mathrm{t}' - \mathrm{k_n}}{\sigma_{\rm n}}\right)^2\right) \tag{17}$$

$$\underset{\mathrm{n}=1,2}{\sigma_{\rm n}} = \alpha_{\rm n} + \beta_{\rm n}\mathrm{t}' \tag{18}$$

and

$$\underset{\mathrm{n}=1,2}{\mathcal{G}_{\mathrm{n}+2}} = \frac{1}{\sqrt{2\pi}\frac{\mathrm{x_n}+\mathrm{y_n}}{2}} \exp\left(-\frac{1}{2}\left(\frac{\mathrm{t} - \varphi_{\rm n}}{\sigma_{\mathrm{n}+2}}\right)^2\right) \tag{19}$$

$$\underset{\mathrm{n}=1,2}{\sigma_{\mathrm{n}+2}} = \begin{cases} \mathrm{x_n} & \text{if } \mathrm{t_i} - \varphi_{\rm n} > 0 \\ \mathrm{y_n} & \text{if } \mathrm{t_i} - \varphi_{\rm n} < 0 \end{cases} \tag{20}$$

where

$$\vec{a_s} = \{g, h, f, j_{1,2}, k_{1,2}, \alpha_{1,2}, \beta_{1,2}, \varphi_{1,2}, x_{1,2}, y_{1,2}, w\} \; . \tag{21}$$

Two of the Gaussians, $\mathcal{G}_1$ and $\mathcal{G}_2$, parameterise a non-zero difference between the reconstructed and true decay times and include widths and means that vary linearly with true decay time. The other two Gaussians, $\mathcal{G}_3$ and $\mathcal{G}_4$, are independent of true decay time and have asymmetric widths to account for the difference in tails to negative and positive reconstructed decay times. The term $\exp(-w\,t')$ allows the contribution from $\mathcal{G}_{3,4}$ to be reduced as the true decay time increases. When the true decay time is large there will be many tracks with significant impact parameters and so it is less likely that a secondary vertex will be reconstructed near the primary vertex.

The parametrisation of the reconstructed decay time distributions was performed using a maximum likelihood fitting technique. For example, at $t' = 1.6$ ps, the value of $f\exp(-w\,t')$ was fitted to be 0.19, the values of σ_1 and σ_2 were 0.29 ps and 0.79 ps, respectively, with $g = 0.52$. Figure 5 shows the reconstructed decay time in six slices of true decay time and the parametrisations from the resolution function are overlaid. Imperfections in the parametrisation are visible, but it was found to be difficult to improve the agreement without a considerable increase in the complexity of the parametrisation. These imperfections are a source of systematic error for the likelihood fit.

7.3 Background Resolution Function

The distribution of reconstructed decay times from background sources (predominantly u,d,s or c quarks on the awayside of a b-tag) is shown in figure 6. A background resolution function, $\mathcal{R}_{\rm bkgd}$, consisting of four normalised Gaussians each centred around a unique reconstructed decay time, accurately describes the distribution of reconstructed decay times from background sources :

$$\mathcal{R}_{\rm bkgd}(t_i, \vec{a_b}) = q\Big(r\,\mathcal{G}_1' + (1-r)\,\mathcal{G}_3'\Big) + (1-q)\Big(s\,\mathcal{G}_2' + (1-s)\,\mathcal{G}_4'\Big), \tag{22}$$

where

$$\underset{n=1,4}{\mathcal{G}_n'} = \frac{1}{\sqrt{2\pi}\,\sigma_n}\,\exp\left(-\frac{1}{2}\left(\frac{t_i - \chi_n}{\sigma_n}\right)^2\right), \tag{23}$$

and

$$\vec{a_b} = \{q, r, s, \sigma_{1,4}, \chi_{1,4}\}. \tag{24}$$

Figure 6 shows the parametrisation of the reconstructed time distribution from background sources. The parametrisation agrees well with the data points. The reconstructed time distribution is centred around zero.

8 Fit to Data/Monte Carlo

Inaccuracies in the parametrisation of the resolution function represent a problem for the likelihood fit described in the previous section. This problem may be overcome by dividing the binned time distribution observed for data by that seen in Monte Carlo, and by fitting the resulting distribution to the ratio of predicted distributions for data and Monte Carlo as a function of the lifetime assumed for data. The binned predicted distributions are calculated from $\mathbb{P}(t_i; \tau_b, \vec{a})$, defined for the likelihood fit, integrated over the bin size.

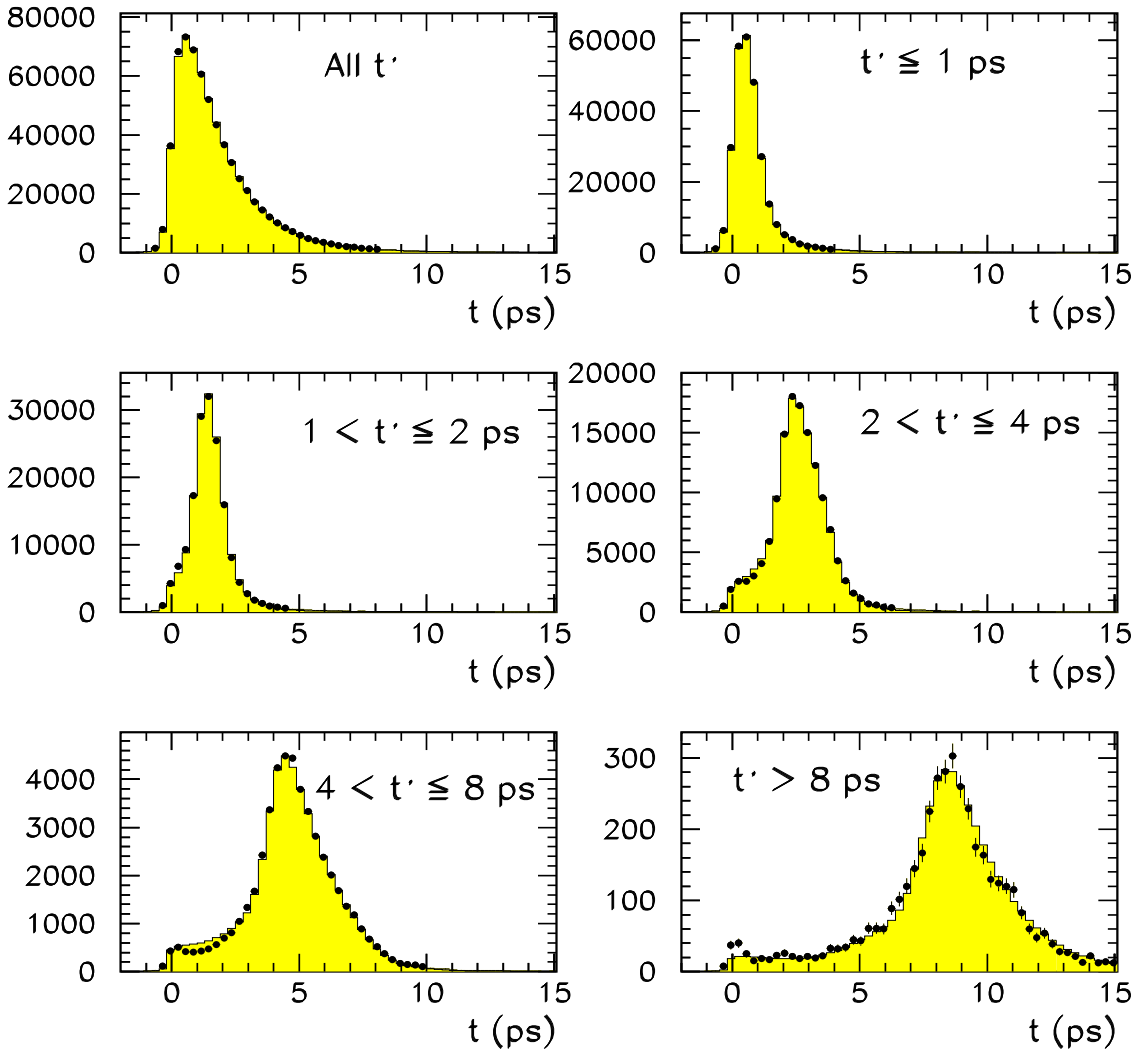

Figure 5: Distributions of the reconstructed decay time shown for different slices of true decay time for signal events. The points represent Monte Carlo data and the solid histogram is the fit from the signal resolution function.

In detail, a χ^2 fit was performed between the quantities $\mathbb{S}$ and $\mathbb{L}$:

$$\mathbb{S} = \frac{\mathrm{S_{data}}}{\mathrm{S_{mc}}}, \tag{25}$$

$$\mathbb{L} = \frac{\mathrm{L_{data}}}{\mathrm{L_{mc}}(\tau = 1.571\,\mathrm{ps})}; \tag{26}$$

where, $\mathrm{S_{mc(data)}}$ and $\mathrm{L_{mc(data)}}$ denote the reconstructed decay time distributions and likelihood predictions from Monte Carlo (data). In such a fit, the parametrisation uncertainties should be suppressed by a factor of about $(\tau_{\mathrm{data}} - \tau_{\mathrm{mc}})/\tau_{\mathrm{mc}}$, where τ_{data} is the fitted lifetime, and τ_{mc} is the lifetime in Monte Carlo.

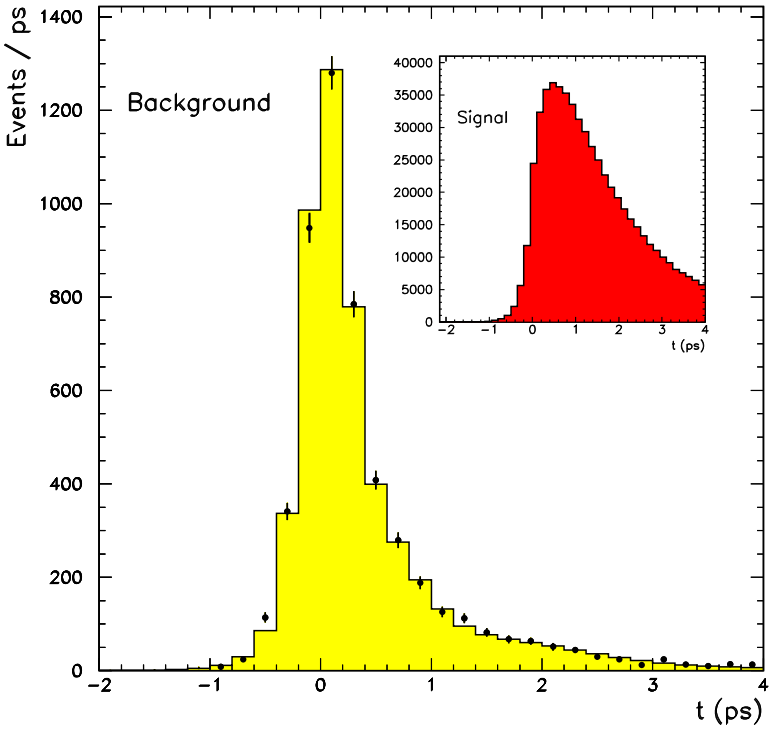

Figure 6: The reconstructed decay time distribution for background events. The points represent Monte Carlo data and the solid histogram is the fit from the background resolution function. The distribution of reconstructed decay times for signal events is also shown for comparison. The background forms approximately 4% of the total sample.

MC Type	N_{ev}	<-5 ps	>25 ps	z	τ_{fit}	τ_{mc}
Default	137 935	0	121	0.964	1.561±0.006	1.571
Unsmeared	103 048	0	86	0.979	1.572±0.007	1.571
Modified frag.	70 248	0	68	0.968	1.581±0.009	1.571

Table 2: The properties of the three Monte Carlo samples used in this analysis. The lifetime fitted from each sample, τ_{fit}, is also shown.

9 Results

The likelihood fit for τ_b was tested on Monte Carlo samples. To provide a test environment as close to data as possible, neural network b-tagging was used to provide a sample enhanced in $Z^0 \rightarrow b\bar{b}$ events. Three Monte Carlo samples are used, as shown in table 2. The reconstructed decay time distributions are divided into 200 bins from -5→25 ps. The numerical integration over true decay time was performed over the range 0→20 ps. Table 2 details : the total number of events in the lifetime fit, N_{ev}; the number of events falling outside the binning range; the proportion of signal events (derived from Monte Carlo 'cheat' information), z; the fitted lifetime, τ_{fit}, and the generated lifetime, τ_{mc}. The resolution and bias functions were re-evaluated using the relevant Monte Carlo sample in each test. The fitted lifetime is close to the generated lifetime in each case, indicating that the parametrisation inaccuracies have only a minor effect on the fitted lifetime. The parametrised reconstructed decay time distribution for the default Monte

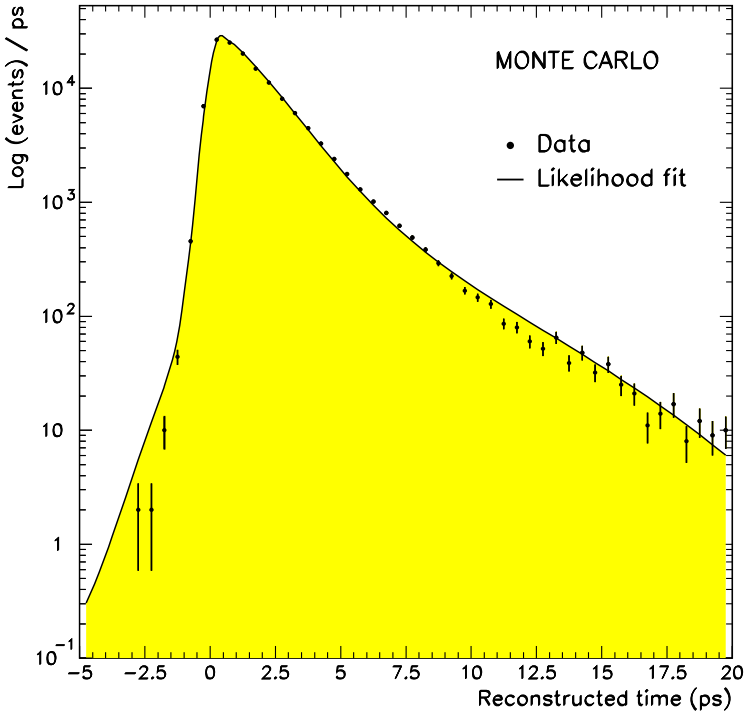

Figure 7: The reconstructed decay time distribution for Monte Carlo data, including backgrounds. The solid line is the result of the lifetime fit.

b Hadron	Generated Sample	Fitted Sample
B meson	92.5%	$(93.3 \pm 0.1)\%$
B^0	43.4%	$(43.1 \pm 0.1)\%$
$B^{\pm}$	43.5%	$(44.4 \pm 0.1)\%$
B_s^0	13.1%	$(12.5 \pm 0.1)\%$
b baryon	7.5%	$(6.7 \pm 0.1)\%$
Λ_b^0	84.5%	$(87.0 \pm 0.3)\%$
Ξ_b^-	7.5%	$(6.4 \pm 0.2)\%$
Ξ_b^0	8.0%	$(6.6 \pm 0.4)\%$

Table 3: The composition of the b hadron sample in Monte Carlo. The generated and fitted sample (after all selection requirements) compositions are shown.

Carlo sample is shown in figure 7. The b hadron composition of the fitted sample was compared to the original mix in the default Monte Carlo, to check for biases towards a particular b hadron species. The results given in table 3 show there is only a small bias in the fitted sample.

The likelihood fit for τ_b was performed on the 95 620 reconstructed decay times in the 1991–1994 data set, using the same binning and integration ranges as described above for the Monte Carlo fits. There was one reconstructed decay time < -5 ps and 76 reconstructed decay times > 25 ps. Using $z = 0.956 \pm 0.006$, as described in section 7, the result of the fit was :

$$\tau_b = (1.590 \pm 0.007)\,\text{ps}, \tag{27}$$

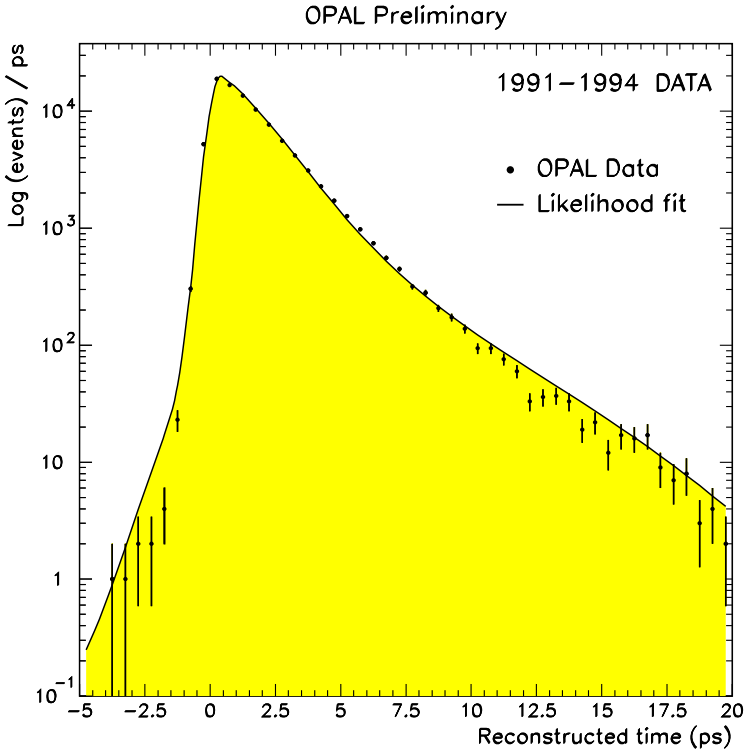

Figure 8: The reconstructed decay time distribution in data. The solid line is the result of the lifetime fit.

where the error is purely statistical. The reconstructed decay time distribution is shown in figure 8.

Finally, the χ^2 fit between $\mathbb{S}$ (data/Monte Carlo) and $\mathbb{L}$ was performed as discussed in section 8, giving

$$\tau_b = (1.597 \pm 0.010)\,\mathrm{ps}, \tag{28}$$

with $\chi^2 = 28.6$ for 17 degrees of freedom, where discrepancies are concentrated in the region $t < 1$ ps. The distribution of $\mathbb{S}$ is shown in figure 9 together with the prediction, $\mathbb{L}$. The agreement is much improved over that seen in figures 7 and 8. This result is adopted as the central value for this paper.

10 Studies of Systematic Errors

Systematic errors may arise from imperfections in the modelling of b fragmentation and the simulation of the lifetime bias and impact parameter resolution in Monte Carlo. Further uncertainties follow from the knowledge of the background, and from uncertainties in the alignment of the silicon detector.

Firstly, uncertainties in the Monte Carlo b fragmentation modelling were studied. Such uncertainties predominantly affect the b hadron energy estimate and therefore the parametrisation of the resolution function. Figure 2 shows that the reconstructed b hadron energy in Monte Carlo and data agree well. As a first check, the reconstructed b energy distribution in Monte Carlo is reweighted to that observed in data. The signal resolution function is parametrised using this new sample of true and reconstructed decay times and the resultant change in the

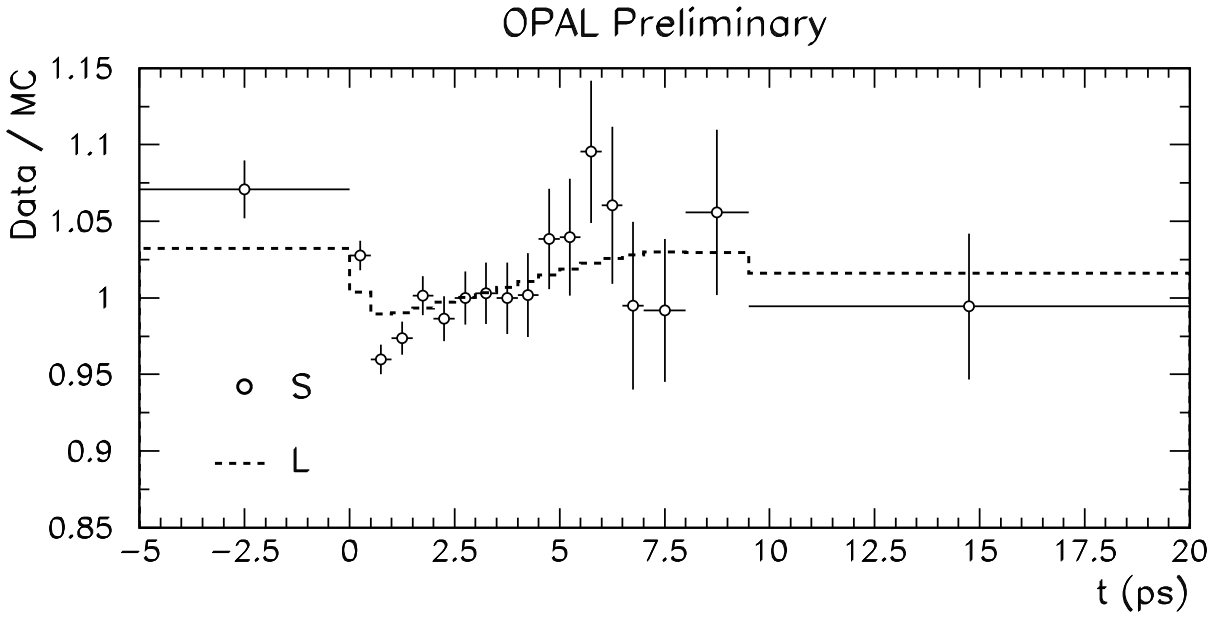

Figure 9: The distribution of data/Monte Carlo for data-points ($\mathbb{S}$) and the likelihood prediction ($\mathbb{L}$).

fitted lifetime was 0.002 ps. Secondly, the reconstructed b energy distribution in Monte Carlo is reweighted to that observed in the Monte Carlo with modified fragmentation parameters. When the resulting resolution function is used to fit the data, the fitted lifetime shift of 0.023 ps is fully consistent with the result obtained using the resolution function obtained from the modified fragmentation Monte Carlo directly. The deviation of 0.023 ps is scaled by 0.36 to account for a one standard deviation shift in $\langle x_E \rangle$ compared to recent measurements (described in section 3), to give 0.008 ps. The total systematic error assigned to uncertainties in the b fragmentation is the quadrature sum of the two effects, 0.008 ps.

In order to test systematic effects due to uncertainties in the background, bias function and also the resolution function, the fitted value of τ_b was studied as a low cut-off on the reconstructed decay time was increased from -5 ps up to 4 ps. The result of this study is shown in Figure 10. The resulting values of τ_b are consistent with the central value across the full time range. However, a systematic error is assigned from the difference between the fitted central value and the value of τ_b at a low cut-off of 1 ps, added in quadrature with the statistical error on this difference. Both the background and the bias function are thought to contribute a negligible uncertainty to the reconstructed time distribution above 1 ps, as indicated in figures 4 and 6, respectively. The resulting systematic error is determined to be ± 0.015 ps.

This error should partly cover also the uncertainties in the signal resolution function due to uncertainties in the Monte Carlo modelling of the impact parameter resolution for charged tracks, but, to be conservative, a separate estimate of this systematic error was assigned. To investigate this source of uncertainty, the resolution functions were parametrised using the unsmeared Monte Carlo sample. This resulted in a fitted lifetime that was increased by 0.031 ps relative to the central value. Since this Monte Carlo sample fails to describe tails of impact parameter distributions, one half of the deviation was assigned as a systematic uncertainty. An alternate smearing algorithm [18] gave consistent results.

A lifetime error of ± 0.008 ps was assigned due to the uncertainty on the proportion of signal events, z. This was estimated using one standard deviation errors on the value of z derived from double tagging with corrections from Monte Carlo, $z_{data} = 0.956 \pm 0.006$. To include such a

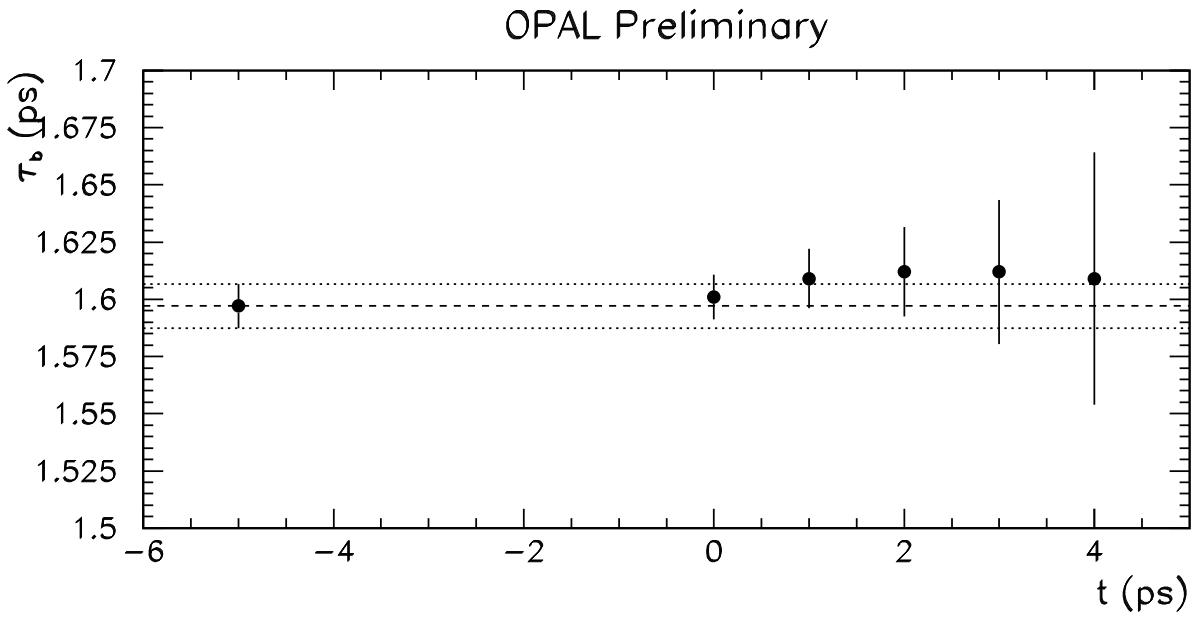

Figure 10: The value of τ_b from the χ^2 fit for various minimum values of reconstructed time, using the $\mathbb{S}/\mathbb{L}$ formalism described in the text. The horizontal band represents the lifetime and error determined using the default time cut-off of -5 ps.

systematic error may be double counting, since the background uncertainty is also covered by the comparison with the result for times larger than 1 ps. No explicit systematic error on C_b was considered other than that due to Monte Carlo statistics. In addition, to account for possible uncertainties in the composition of the background (predominantly due to c or u, d or s quarks), the background resolution function was reparametrised reducing the contribution from u, d and s quarks by a factor of two. All other parameters in the lifetime fit were left unchanged. A systematic error of ± 0.003 ps was assigned to account for the change in fitted lifetime.

Alignment studies indicate that the radial position of the silicon detectors is known to within 50 μm. This could introduce a systematic effect in the determination of the b hadron decay length. The effect is modelled by shifting both layers of silicon detectors coherently and re-determining the decay length. A shift in the mean reconstructed decay time of 0.0045 ± 0.0015 ps was observed and a conservative systematic error of ± 0.006 ps was therefore assigned to this source of uncertainty.

As a cross-check of the overall method, the data set was divided into four years (1991–1994) and each year was fitted separately. Data from 1991 to 1994 made up approximately 8%, 26%, 21% and 45%, respectively, of the total data-set. The value of z derived for each year, from the double tagging technique with associated Monte Carlo corrections, is shown in table 4 with the corresponding fitted lifetime. The error weighted average of individual lifetime results from each year is consistent with the central lifetime result. The χ^2 per degree of freedom between the individual lifetime results and the combined result is 2.9, which corresponds to a probability of 3.5%. If the statistical error on z is taken into account for each year, then the χ^2 per degree of freedom is reduced to 2.1, with a probability of 9.4%. When the same test is performed with a low cut-off of 1 ps, the agreement is excellent: $\chi^2 = 0.19$ per degree of freedom. Thus any potential systematic problem would seem to be already covered by the comparison with the result for times greater than 1 ps.

The systematic errors are summarised in table 5.

Year	Signal Proportion, z (%)	τ_b (ps)
1991	94.8 ± 1.3	1.534 ± 0.028
1992	95.3 ± 0.7	1.593 ± 0.016
1993	95.8 ± 0.7	1.584 ± 0.017
1994	95.7 ± 0.6	1.614 ± 0.013
1991–4 (w.a.)	95.6 ± 0.4	1.596 ± 0.010
1991–4 (full)	95.6 ± 0.4	1.597 ± 0.010

Table 4: The value of the signal proportion, z, evaluated for each year of data-taking using a double tagging technique. The resulting fitted value of τ_b is also shown. The indicated errors on both z and τ_b are purely statistical. The z and τ_b results for 1991–1994 are from an error weighted average of each individual year (w.a.) and a fit to all four years together (full).

Source of Uncertainty	Systematic Error (ps)
b fragmentation	± 0.008
Background and bias correction function	± 0.015
Modelling of impact parameter resolution	± 0.016
Signal proportion	± 0.008
Background composition	± 0.003
Silicon detector alignment	± 0.006
Total	± 0.026

Table 5: A summary of the systematic errors assigned to τ_b.

11 Conclusions

Approximately 3.5 million hadronic events recorded by the OPAL detector between 1991 and 1994 have been used to measure τ_b. These events have been used to reconstruct 95 620 b hadron decay times. The b hadron decay time is reconstructed from measurements of the b hadron decay length and momentum. A fit to the ratio of the reconstructed time distributions seen in data and Monte Carlo is used to extract

$$\tau_b = (1.597 \pm 0.010\,(\text{stat}) \pm 0.026\,(\text{syst}))\,\text{ps}. \tag{29}$$

The largest contributions to the systematic error result from the Monte Carlo modelling of impact parameter resolutions, the bias due to selection criteria and background.

The current world average is $\tau_b = (1.549 \pm 0.020)$ ps [11]. The result presented in this paper is compatible with this to 1.4 standard deviations, assuming uncorrelated systematic errors, and has a competitive precision. We also note that results have been obtained by the DELPHI and SLD collaborations [3] using inclusively reconstructed secondary vertices. They measure : $\tau_b = (1.582 \pm 0.011\,(\text{stat}) \pm 0.027\,(\text{syst}))\,\text{ps}$ and $\tau_b = (1.564 \pm 0.030\,(\text{stat}) \pm 0.036\,(\text{syst}))\,\text{ps}$, respectively, in good agreement with the result presented here.

References

[1] L3 Collaboration, O. Adriani et al., Phys. Lett. **B317** (1993) 474;
ALEPH Collaboration, D. Buskulic et al., Phys. Lett. **B369** (1996) 151;
DELPHI Collaboration, P. Abreu et al., Z. Phys. **C63** (1994) 3.

[2] OPAL Collaboration, P.D. Acton et al., Z. Phys. **C60** (1993) 217.

[3] DELPHI Collaboration, P. Abreu et al., CERN-PPE/96-013, submitted to Phys. Lett. **B**;
SLD Collaboration, K. Abe et al., Phys. Rev. Lett. **75** (1995) 3624.

[4] OPAL Collaboration, K. Ahmet et al., Nucl. Instr. Meth. **A305** (1991) 275.

[5] O. Biebel et al., Nucl. Instr. and Meth. **A323** (1992) 169;
M. Hauschild et al., Nucl. Instr. and Meth. **A314** (1992) 74.

[6] P.P. Allport et al., Nucl. Instr. Meth. **A324** (1993) 34.

[7] P.P. Allport et al., Nucl. Instr. Meth. **A346** (1994) 476.

[8] OPAL Collaboration, G. Alexander et al., Z. Phys. **C52** (1991) 175.

[9] T. Sjöstrand, Comp. Phys. Comm. **82** (1994) 74.

[10] OPAL Collaboration, G. Alexander et al., Z. Phys. **C69** (1996) 543.

[11] The Particle Data Group, R.M. Barnett et al., Phys. Rev. **D54** (1996) 1.

[12] C. Peterson, D. Schlatter, I. Schmitt and P. Zerwas, Phys. Rev. **D 27** (1983) 105.

[13] OPAL Collaboration, G. Alexander et al., Phys. Lett. **B364** (1995) 93;
ALEPH Collaboration, D. Buskulic et al., Phys. Lett. **B357** (1995) 699.

[14] J. Allison et al., Nucl. Instr. and Meth. **A317** (1992) 47.

[15] OPAL Collaboration, R. Akers et al., Z. Phys. **C61** (1994) 209.

[16] OPAL Collaboration, R. Akers et al., Z. Phys. **C66** (1995) 19.

[17] OPAL Collaboration, R. Akers et al., Z. Phys. **C68** (1995) 179.
The jet finding parameters ϵ and R were set to 5.0 GeV and 0.65, respectively.

[18] OPAL Collaboration, R. Akers et al., Z. Phys. **C65** (1995) 17.

[19] L. Montanet et al., Phys. Rev. **D50** (1994) 1173.

[20] OPAL Collaboration, P.D. Acton et al., Phys. Lett. **B273** (1991) 355.

[21] OPAL Collaboration, R. Akers et al., Z. Phys. **C66** (1995) 555.

[22] OPAL Collaboration, R. Akers et al., Z. Phys. **C66** (1995) 19.